Proposal for an ac spin current source

Patrick P. Hofer [(a)1], Hugo Aramberri[2], Christoph Schenke[1] and Pierre A. L. Delplace[1]

[1] *Département de Physique Théorique, Université de Genève - CH-1211 Genève 4, Switzerland*
[2] *Instituto de Ciencia de Materiales de Madrid (ICMM-CSIC) - Cantoblanco 28049 Madrid, Spain*

arXiv:1403.6674v1 [cond-mat.mes-hall] 26 Mar 2014

PACS 72.10.-d – Theory of electronic transport; scattering mechanisms
PACS 85.75.-d – Magnetoelectronics; spintronics: devices exploiting spin polarized transport or integrated magnetic fields
PACS 73.43.-f – Quantum Hall effects

Abstract – We propose an ac current source that can be tuned from a pure *charge* to a pure *spin* current source. The device consists of two mesoscopic capacitors attached to a two-dimensional strip of a topological insulator. The change from charge to spin current is controlled by an offset in the top gate potentials that drive the capacitors. In addition to this setup, which anticipates the experimental realisation of quantum point contacts in topological insulators, we propose an analogous source in the quantum Hall regime which only relies on presently available building blocks. To this end, we calculate the band structure of a topological insulator in a magnetic field. The intrinsic spin-orbit coupling, together with a split gate, allows for an analogous source, where charge and spin current can be manipulated. The realisation of the device as well as the detection of the ac spin current are within reach of present experimental technology.

Introduction. – Topological insulators (TI) are states of matter which are not characterised by a local order parameter but by a topological invariant that represents a global order of the system [1–4]. At the interface between materials featuring different topological invariants, localised states appear. In particular, two-dimensional TIs which are invariant under time reversal (TR) exhibit pairs of helical edge states at interfaces to topologically trivial insulators such as the vacuum. The members of these pairs are related by TR and thus propagate in opposite directions and have opposite spin. As supported by recent experiments [5–11], the topological nature of these states ensures the absence of backscattering as long as interactions and inelastic processes are negligible. These properties make edge channels in TIs the ideal candidates for electron waveguides in spintronics applications.

The field of spintronics strives for control and manipulation of the spin degrees of freedom in condensed matter systems [12]. Spintronics devices can in general be used as logical base units for high performance computation and their main ingredients are spin transistors and spin filters, based on the spin valve effect [13, 14]. Such devices have been realised in various nanostructures, e.g., ferromagnetic tunnel junctions, molecules, and carbon nanotubes [15–18]. More recently, proposals which use the spin polarised edge modes of TIs in order to create spin filters, spin transistors, and spin current pumps [19–22] have attracted attention. Particularly promising are logic devices which suggest computation schemes with low power consumption [23–25].

Another promising route towards energy efficient computation is provided by electronic few particle processes. Using sources that emit single particles on demand [26–29], pioneering experiments [30–35] proved the feasibility of creating and manipulating single electron excitations in a controlled manner.

In this Letter, we propose to use two single-particle sources provided by mesoscopic capacitors [27] to emit electrons and holes into the helical edge states of a TI [36, 37]. Thereby an ac current in the GHz range is produced that can be tuned from a pure charge to a pure spin current. Recent experiments reporting on the detection of ac spin currents in the GHz range [38–41] stress the experimental importance of the field of ac spintronics [42, 43]. A device where a dc current can be tuned from a spin-polarised charge current to a pure spin current is discussed in Ref. [44].

Because of spin-orbit coupling, spin is usually not a good quantum number in the considered systems. The

(a) E-mail: patrick.hofer@unige.ch

role of spin and total angular momentum is clarified below. The single-particle sources rely on quantum point contacts (QPC), which represent a considerable experimental challenge in TIs. To circumvent this, we additionally propose a setup where the TI is tuned into the quantum Hall (QH) regime by a strong magnetic field. For this setup, all the building blocks are presently available. The quantitative analysis of our proposal is done using material parameters of experimentally available TIs [9]. Due to the strong intrinsic spin-orbit coupling that mediates the band inversion in these TIs, the device still acts as a source of pure spin current although TR symmetry is explicitly broken.

The rest of the Letter is structured as follows. First we discuss the edge states in the utilised model, focusing on their spin and angular momentum polarisation. The next section is dedicated to the proposed device in the quantum spin Hall regime. We then present the behaviour of the band structure in a magnetic field, providing the necessary background for the following discussion of the setup in the QH regime. We end the letter with a summary and concluding remarks.

BHZ model. – The model we employ for a two-dimensional TI was developed by Bernevig, Hughes and Zhang (BHZ) [45]. The resulting Bloch-Hamiltonian reads

$$\begin{aligned} H(\boldsymbol{k}) &= \begin{pmatrix} h(\boldsymbol{k}) & 0 \\ 0 & h^*(-\boldsymbol{k}) \end{pmatrix}, \\ h(\boldsymbol{k}) &= \epsilon(\boldsymbol{k})\mathbb{1}_2 + \boldsymbol{d}(\boldsymbol{k})\cdot\boldsymbol{\sigma}, \qquad \epsilon(\boldsymbol{k}) = \tilde{C} - \tilde{D}k^2 \\ \boldsymbol{d}(\boldsymbol{k}) &= [\tilde{A}k_x, -\tilde{A}k_y, M(\boldsymbol{k})], \qquad M(\boldsymbol{k}) = \tilde{M} - \tilde{B}k^2, \end{aligned} \tag{1}$$

where the quantities with a tilde are material specific parameters, $\mathbb{1}_2$ is the identity matrix of order 2, $\boldsymbol{\sigma}$ is the vector of Pauli matrices and $k^2 = k_x^2 + k_y^2$. Systems that are described by this Hamiltonian include quantum wells of HgTe/CdTe [45], InAs/GaSb [46] and Ge/GaAs [47]. The basis states of the BHZ Hamiltonian are denoted by $(|E,+1/2\rangle, |H,+3/2\rangle, |E,-1/2\rangle, |H,-3/2\rangle)$, where E (H) denotes states derived from electron-like (hole-like) bands and the number gives m_j, the projection of the total angular momentum on the z-axis. These basis states are discussed in detail in Refs. [48, 49]. Importantly, m_j is a good quantum number for the basis states and does not depend on the specific material or sample geometry. We therefore discuss the proposed device as a source of total angular momentum current. The projection of the electron spin onto the z-axis, m_s, is only a good quantum number for the states $|H,\pm3/2\rangle$ which have $m_s = \pm1/2$. However, in the case of HgTe/CdTe, one can make an estimate of the spin polarisation of the $m_j = \pm1/2$ states based on Ref. [49], which gives $\langle E,\pm1/2|\, S_z\, |E,\pm1/2\rangle \approx \pm0.73\hbar/2$ for a well-width of 7 nm. Here, S_z is the z-component of the electron-spin operator. For all basis states, we thus find that $\langle S_z\rangle$ and m_j have equal signs, which means that the currents associated with these two quantities are proportional to each other. This justifies the notion of spin current although we discuss the source in terms of total angular momentum current which is sample and material independent unlike the electron-spin current.

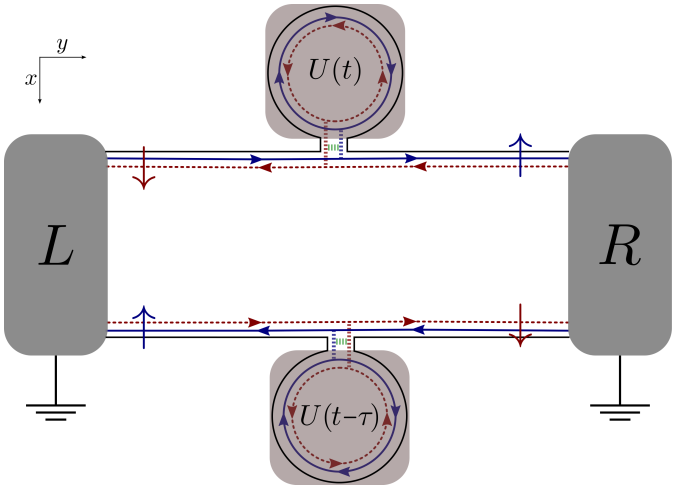

Fig. 1: Proposed ac spin current source in the topological insulator regime. Two mesoscopic capacitors are attached to a two-dimensional topological insulator. If they are operated in phase ($\tau = 0$), they both emit electrons and holes at equal times resulting in a pure and equal ac *charge* current in the two contacts (R/L). A delay, τ, can synchronise electron and hole emission on the different edges. This results in a pure ac *spin* current of opposite sign in the different contacts. The arrows indicate the expectation value of the spin.

We refer to the eigenstates of the upper (lower) block of Eq. (1) as spin up (down) states. The edge modes can be found by solving the Hamiltonian for hard wall boundary conditions [50, 51]. Since they have equal weights on the $|E,\pm1/2\rangle$ and $|H,\pm3/2\rangle$ state, we find $\langle J_z\rangle_\alpha = \pm\hbar$, where J_z is the z-component of the total angular momentum operator and α labels the spin of the edge state. Tuning the Fermi energy, E_F, into the bulk gap, only these edge modes contribute to transport. They constitute the scattering channels which are referred to below.

Time reversal invariant source. – The proposed source is sketched in Fig. 1. It consists of two mesoscopic capacitors attached to opposite sides of a strip of a two-dimensional TI. The working principle of a mesoscopic capacitor in the TI regime is discussed in Refs. [36, 37] and is similar to the analogous device in the QH regime [27], which has been implemented experimentally [30]. A mesoscopic capacitor consists of a quantum dot, tunnel coupled to the helical edge states. Using a top gate, $U(t)$, a pair of Kramers degenerate quantum dot levels are moved above and below E_F in a periodic manner. Every time the Kramers pair is lifted above E_F, one electron is ejected into each outgoing channel, one propagating to the left, one to the right. Every time the level pair moves below E_F a hole is emitted into each channel. A single capacitor thereby creates an equal, spin-polarised ac charge current in the contacts L and R.

For simplicity, identical capacitors are considered, the only difference being a time shift τ in their periodic top gate potential. If the two capacitors are operated in phase ($\tau = 0$), the charge current measured at one of the contacts (R/L) is doubled with respect to a single capacitor but the spin current is cancelled, since there is a channel of each spin entering each contact. Operating the capacitors out of phase, such that electron emission of one capacitor is synchronised with hole emission of the other capacitor, the charge current vanishes. Since an electron of a given spin species and a hole of the opposite spin species contribute equally to the spin current, this results in a pure ac spin current which is opposite in each contact.

For a quantitative analysis, we resort to the scattering approach [26]. There are four channels connecting the two contacts in the setup sketched in Fig. 1. Since the channels at the upper and lower edges are well separated and because of TR invariance, there is no scattering between the channels. The total charge current is therefore just the sum of the currents created by each capacitor. In order to move a dot level above and below E_F, we consider the experimentally relevant step-like top gate potential with an amplitude given by the dot level spacing Δ and a frequency $2\pi/\mathcal{T}$ in the GHz range [34]. As mentioned above, each capacitor separately emits the same (opposite) charge (spin) current into the right- and left-moving channels. The charge current emitted into a single channel by the capacitor located at the upper edge is periodic in time with period $\mathcal{T}$ and reads [28]

$$I^c(t) = \begin{cases} \frac{e}{\tau_D} e^{-t/\tau_D} & \text{for } 0 \le t < \mathcal{T}/2, \\ -\frac{e}{\tau_D} e^{-(t-\mathcal{T}/2)/\tau_D} & \text{for } \mathcal{T}/2 \le t < \mathcal{T}. \end{cases} \tag{2}$$

Here $\tau_D = h/(D\Delta)$ is the dwell time with D being the transmission probability through the QPC and $e < 0$ is the elementary charge. We consider the case where $\tau_D \ll \mathcal{T}/2$, such that in each cycle exactly one electron and one hole is emitted. The charge current emitted by the capacitor located at the lower edge is given by $I^c(t-\tau)$.

Due to the linear dispersion, the spin current in a given channel α is proportional to the charge current $I^s_\alpha(t) = \langle J_z \rangle_\alpha I^c_\alpha / e$. The quantised emission of a single particle into channel α is therefore accompanied by the quantised emission of angular momentum in units of $\langle J_z \rangle_\alpha$. Operating the two capacitors with a time shift τ leads to the currents in the right and left contacts

$$\begin{aligned} I^c_R(t) &= I^c_L(t) = I^c(t) + I^c(t-\tau), \\ I^s_R(t) &= -I^s_L(t) = \frac{\hbar}{e}\left[I^c(t) - I^c(t-\tau)\right], \end{aligned} \tag{3}$$

where the subscript R/L denotes the contact and we made use of the fact that $\langle J_z \rangle_\alpha = \pm\hbar$ for the edge channels (see Fig. 1).

The charge and spin currents entering the right contact are plotted in Fig. 2. For $\tau = 0$, each capacitor emits an electron at time $t = 0$ and a hole at time $t = \mathcal{T}/2$.

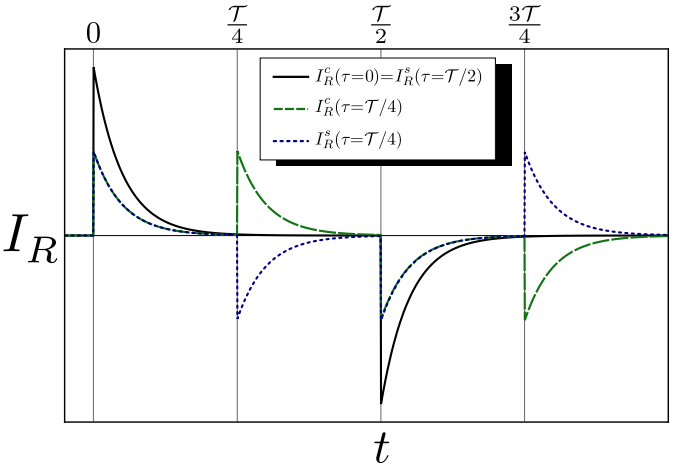

Fig. 2: Charge and spin current ($e = \hbar = 1$) emitted by the source into the right contact. Black (solid) line shows the pure charge current for synchronous operation which is equal to the pure spin current for $\tau = \mathcal{T}/2$. The green (broken) line shows the charge current, the blue (dashed) line the spin current, for a finite delay. Changing τ moves the peaks and dips centred around τ and $\mathcal{T}/2 + \tau$, going from a pure charge ($\tau = 0$) to a pure spin current ($\tau = \mathcal{T}/2$). Note that an equal (opposite) charge (spin) current enters the left contact.

The charge current is thus maximised and there is no spin current. For a finite τ, the upper capacitor emits an electron at time $t = 0$ which contributes positively to both charge and spin current, while the lower capacitor emits an electron at time $t = \tau$ which contributes positively to the charge and negatively to the spin current. The opposite holds for the holes and for the spin current in the left contact. Finally, when $\tau = \mathcal{T}/2$, the electron of the upper capacitor is synchronised with the hole of the lower capacitor. The charge current vanishes and the spin current is maximised. Controlling the time shift thus allows one to tune from a pure charge to a pure spin current. Conveniently, mesoscopic capacitors are usually operated in the GHz range, where experimental detection of ac spin currents has recently been reported [38–41].

Edge states in a magnetic field. – Since the fabrication of QPCs in topological insulators remains an open challenge, we extend our proposal to the QH regime, where QPCs can be implemented using gates. To this end, we first describe the behaviour of the helical edge states in a perpendicular magnetic field. The transition from the quantum spin Hall to the QH regime in graphene is discussed in Ref. [52], the effect of a magnetic field in HgTe/CdTe quantum wells in Refs. [53, 54]. In the light of recent experiments [9, 11], we consider an InAs/GaSb quantum well with the material parameters given in Ref. [55]. Since we are interested in the spin texture, we take into account the spin coupling terms that arise in this material due to bulk (BIA) and structural inversion asymmetry (SIA) [46]

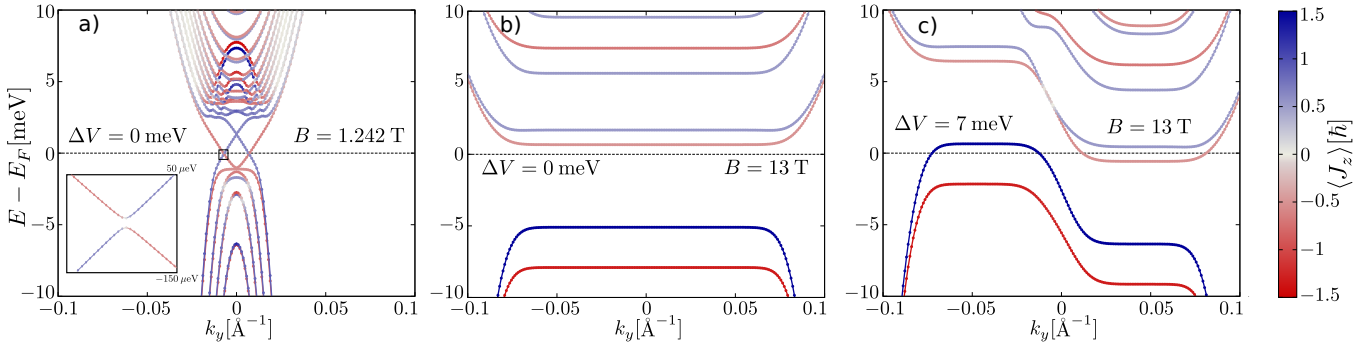

Fig. 3: Evolution of the band structure of InAs/GaSb in a magnetic field. The colour scheme indicates the expectation value $\langle J_z \rangle$. a) For a weak magnetic field, spin up (down) states move up (down) in energy and the crossing of opposite spin states moves to negative (positive) k_y for the upper (lower) edge. The crossings at zero energy are lifted by the inversion asymmetry terms as shown in the inset. b) In a strong magnetic field, Landau levels develop with a characteristic texture of $\langle J_z \rangle$. For fields stronger then B_c, the intrinsic band inversion is revoked and all the electron-like Landau levels are above the hole-like Landau levels. c) A split gate can move the band structure up (down) on the upper (lower) half of the sample by locally applying the potential V_u (V_l), with $\Delta V \equiv V_u - V_l$. This is done in a way that the upper half supports a $\langle J_z \rangle_u = 3\hbar/2$ and the lower half a $\langle J_z \rangle_l = -\hbar/2$ edge channel. For these calculations we used a tight-binding regularization of the BHZ model.

$$H_{\mathrm{BIA}}(\boldsymbol{k}) = \begin{pmatrix} 0 & 0 & \Delta_e k_+ & -\Delta \\ 0 & 0 & \Delta & \Delta_h k_- \\ \Delta_e k_- & \Delta & 0 & 0 \\ -\Delta & \Delta_h k_+ & 0 & 0 \end{pmatrix}, \qquad (4)$$

and

$$H_{\mathrm{SIA}}(\boldsymbol{k}) = \begin{pmatrix} 0 & 0 & iRk_- & 0 \\ 0 & 0 & 0 & 0 \\ -iR^* k_+ & 0 & 0 & 0 \\ 0 & 0 & 0 & 0 \end{pmatrix}, \qquad (5)$$

where $k_\pm = k_x \pm i k_y$ and $\Delta_{e/h}$, R are material dependent constants [55]. We neglect the Zeeman splitting, since it has the same effect as the orbital coupling to the magnetic field but is of much smaller magnitude [50]. The Hamiltonian we consider is thus the sum of Eqs. (1, 4, 5), where the magnetic field is introduced using the minimal coupling in the Landau gauge

$$k_x \to -i\partial_x, \qquad k_y \to k_y - \frac{e}{\hbar} B x. \qquad (6)$$

The behaviour of the edge states in a magnetic field is illustrated in Fig. 3 a and b. For small magnetic fields, the up (down) spin states are pushed up (down) in energy. This shifts the crossing of the opposite spin states at zero energy to negative k_y values for the upper edge and to positive k_y values for the lower edge. Since these crossings are no longer protected by TR invariance and since the spins are coupled by the inversion asymmetry terms, a gap opens up (see inset of Fig. 3 a).

Further increasing the magnetic field moves the crossings between the same spin states into the bulk states. Coupling of the different edges via the bulk states lifts these degeneracies and Landau levels are formed. The spin up states give rise to a hole-like Landau level which is above the electron-like spin-down Landau level due to the intrinsic band inversion (not shown). Since at high magnetic fields, k_y is directly proportional to the x-component of the centre of cyclotron motion, we can read off the localisation of the electrons directly from the band structure. Increasing the magnetic field further shifts the hole-like spin-up level down and the electron-like spin-down level up in energy, until they eventually undergo an avoided crossing at $B_c = \hbar\tilde{M}/(e\tilde{B}) \approx 8.23T$ [50]. For higher magnetic fields, all electron-like Landau levels are above the hole-like Landau levels and they alternate in the sign of $\langle J_z \rangle_\alpha$ (see Fig. 3 b).

We note that although this evolution is qualitatively the same for all systems described by the BHZ model, the different material parameters lead to a quantitative similarity in HgTe/CdTe while in Ge/GaAs the required magnetic fields are two orders of magnitude higher.

Quantum Hall source. – In this section, we extend our proposal to the QH regime, where it consists exclusively of experimentally available building blocks.

A bottom gate can be used to shift the band structure relative to E_F. As experimentally demonstrated in Ref. [7], a split gate can be used to shift the band structure up in energy in one half, and down in energy in the other half of the sample. We model this by including a potential V which is positive in the upper half and negative in the lower half of the sample (see Fig. 4). This leads to the band structure shown in Fig. 3 c with four states at E_F. The states at the edges of the sample both propagate to the right and have spin polarisations of opposite signs but different magnitudes. The state at the upper edge has $\langle J_z \rangle_u = 3\hbar/2$, the state at the lower edge $\langle J_z \rangle_l = -\hbar/2$. Since the leftmoving states are located in the middle of the sample, there is no backscattering.

To achieve a source of ac spin current, a mesoscopic ca-

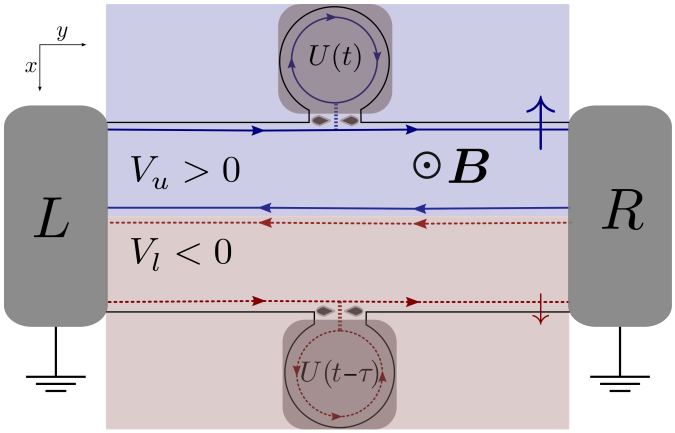

Fig. 4: Proposed ac spin current source in the quantum Hall regime. A strong magnetic field is used to produce Landau levels. Using a split gate (V_u and V_l, blue and red shading), the upper half is tuned into a regime where one edge state with $\langle J_z \rangle_u = 3\hbar/2$ (blue, solid) propagates clockwise, while in the lower half an edge state with $\langle J_z \rangle_l = -\hbar/2$ (red, dashed) propagates counter clockwise. The leftmoving states are localised in the middle of the sample, ensuring the absence of backscattering.

pacitor is attached to each side of the sample as sketched in Fig. 4. The current emitted by the capacitors is described by Eq. (2). Note that in this setup, the channels connected to the mesoscopic capacitors both propagate to the right, meaning that $I_L^c = I_L^s = 0$. The charge current in the right contact is still given by Eq. (3), but since the involved states have different $|\langle J_z \rangle|$, the spin current now reads

$$I_R^s(t) = \frac{\hbar}{e}\left[\frac{3}{2}I^c(t) - \frac{1}{2}I^c(t-\tau)\right]. \qquad (7)$$

Even at $\tau = 0$, this source thus emits a spin current of I^c; a pure charge current can no longer be created. However, a pure spin current of $2I^c$ can still be generated by an offset $\tau = \mathcal{T}/2$.

As shown in Fig. 3 c, the spin down state that is coupled to the lower capacitor has a spin up state in its vicinity. The gap between these states is approximately 1 meV, which corresponds to 12 K. We note that even if the Fermi energy does not lie in this gap but above the spin up Landau level, the QPC of the capacitor can be chosen to be transmitting only for the outer, spin down edge channel. For HgTe/CdTe quantum wells, no other state is in the vicinity of the utilised states.

Conclusion. – Using two mesoscopic capacitors [27] attached to the sides of a TI, we propose an ac current source that can be tuned from a pure *charge* to a pure *spin* current source by varying an offset in the driving potentials of the capacitors. So far, QPCs have not been implemented in TIs. We therefore extend our proposal to the QH regime, where QPCs are provided by gates. To this end, we discuss the behaviour of the helical edge states in a perpendicular magnetic field [53, 54]. The emerging Landau levels have a characteristic angular momentum structure due to the intrinsic spin-orbit coupling of TI materials. Using a split gate [7], we produce a situation where two co-propagating states with angular momentum expectation value of opposite directions are localised at the opposite edges of the sample. Analogous to the source in the TR invariant regime, the charge and spin currents can be manipulated by varying the offset in the driving potentials. Since the magnitude of the angular momentum expectation value on the two edges is different, a pure *charge* current cannot be produced any more. However, a pure ac *spin* current can still be generated.

Due to recent experimental breakthroughs in the fields of single electron sources [30, 33], topological insulators [9, 11], and spin current detection [38–41], our proposal is experimentally feasible and will hopefully stimulate more experiments in the upcoming field of ac spintronics.

* * *

We acknowledge the involvement of Markus Büttiker at an early stage of this project. We thank Gwendal Fève for helpful discussions. All numerical calculations were done using the MOJITO code written by Jian Li, whom we also thank for stimulating discussions.

This research is supported by the SNSF. H.A. acknowledges support from the Spanish Ministerio de Ciencia e Innovacion (MICINN) through the Grant No. MAT2009-14578-C03-03.

REFERENCES

[1] Bernevig B. A. and Hughes T. L., *Topological Insulators and Topological Superconductors* (Princeton University Press) 2013.
[2] Kane C. L. and Mele E. J., *Phys. Rev. Lett.*, **95** (2005) 146802.
[3] Hasan M. Z. and Kane C. L., *Rev. Mod. Phys.*, **82** (2010) 3045.
[4] Qi X.-L. and Zhang S.-C., *Rev. Mod. Phys.*, **83** (2011) 1057.
[5] König M., Wiedmann S., Brüne C., Roth A., Buhmann H., Molenkamp L. W., Qi X.-L. and Zhang S.-C., *Science*, **318** (2007) 766.
[6] Roth A., Brüne C., Buhmann H., Molenkamp L. W., Maciejko J., Qi X.-L. and Zhang S.-C., *Science*, **325** (2009) 294.
[7] Brüne C., Roth A., Buhmann H., Hankiewicz E. M., Molenkamp L. W., Maciejko J., Qi X.-L. and Zhang S.-C., *Nat Phys*, **8** (2012) 485.
[8] Grabecki G., Wróbel J., Czapkiewicz M., Cywiński L., Gierałtowska S., Guziewicz E., Zholudev M., Gavrilenko V., Mikhailov N. N., Dvoretski S. A., Teppe F., Knap W. and Dietl T., *Phys. Rev. B*, **88** (2013) 165309.
[9] Du L., Knez I., Sullivan G. and Du R.-R., *Observation of quantum spin Hall states in InAs/GaSb bilayers under broken time-reversal symmetry*, arXiv:1306.1925 (2013).

[10] Suzuki K., Harada Y., Onomitsu K. and Muraki K., *Phys. Rev. B*, **87** (2013) 235311.

[11] Spanton E. M., Nowack K. C., Du L., Du R.-R. and Moler K. A., *Images of edge current in InAs/GaSb quantum wells*, arXiv:1401.1531 (2014).

[12] Žutić I., Fabian J. and Das Sarma S., *Rev. Mod. Phys.*, **76** (2004) 323.

[13] Julliere M., *Phys. Lett. A*, **54** (1975) 225 .

[14] Slonczewski J. C., *Phys. Rev. B*, **39** (1989) 6995.

[15] Schelp L. F., Fert A., Fettar F., Holody P., Lee S. F., Maurice J. L., Petroff F. and Vaurès A., *Phys. Rev. B*, **56** (1997) R5747.

[16] Pasupathy A. N., Bialczak R. C., Martinek J., Grose J. E., Donev L. A. K., McEuen P. L. and Ralph D. C., *Science*, **306** (2004) 86.

[17] Cottet A., Kontos T., Sahoo S., Man H. T., Choi M.-S., Belzig W., Bruder C., Morpurgo A. F. and Schönenberger C., *Semicond. Sci. Technol.*, **21** (2006) S78.

[18] Man H. T., Wever I. J. W. and Morpurgo A. F., *Phys. Rev. B*, **73** (2006) 241401.

[19] Maciejko J., Kim E.-A. and Qi X.-L., *Phys. Rev. B*, **82** (2010) 195409.

[20] Krueckl V. and Richter K., *Phys. Rev. Lett.*, **107** (2011) 086803.

[21] Dolcetto G., Cavaliere F., Ferraro D. and Sassetti M., *Phys. Rev. B*, **87** (2013) 085425.

[22] Mahfouzi F., Nikolić B. K., Chen S.-H. and Chang C.-R., *Phys. Rev. B*, **82** (2010) 195440.

[23] Datta S. and Das B., *Appl. Phys. Lett.*, **56** (1990) 665.

[24] Wolf S. A., Awschalom D. D., Buhrman R. A., Daughton J. M., von Molnr S., Roukes M. L., Chtchelkanova A. Y. and Treger D. M., *Science*, **294** (2001) 1488.

[25] Behin-Aein B., Datta D., Salahuddin S. and Datta S., *Nat. Nanotechnol.*, **5** (2010) 266.

[26] Moskalets M. V., *Scattering matrix approach to non-stationary quantum transport* (Imperial College Press) 2012.

[27] Moskalets M., Samuelsson P. and Büttiker M., *Phys. Rev. Lett.*, **100** (2008) 086601.

[28] Keeling J., Shytov A. V. and Levitov L. S., *Phys. Rev. Lett.*, **101** (2008) 196404.

[29] Keeling J., Klich I. and Levitov L. S., *Phys. Rev. Lett.*, **97** (2006) 116403.

[30] Fève G., Mahé A., Berroir J.-M., Kontos T., Plaçais B., Glattli D. C., Cavanna A., Etienne B. and Jin Y., *Science*, **316** (2007) 1169.

[31] Mahé A., Parmentier F. D., Bocquillon E., Berroir J.-M., Glattli D. C., Kontos T., Plaçais B., Fève G., Cavanna A. and Jin Y., *Phys. Rev. B*, **82** (2010) 201309.

[32] Bocquillon E., Parmentier F. D., Grenier C., Berroir J.-M., Degiovanni P., Glattli D. C., Plaçais B., Cavanna A., Jin Y. and Fève G., *Phys. Rev. Lett.*, **108** (2012) 196803.

[33] Bocquillon E., Freulon V., Berroir J.-M., Degiovanni P., Plaçais B., Cavanna A., Jin Y. and Fève G., *Science*, **339** (2013) 1054.

[34] Parmentier F. D., Bocquillon E., Berroir J.-M., Glattli D. C., Plaçais B., Fève G., Albert M., Flindt C. and Büttiker M., *Phys. Rev. B*, **85** (2012) 165438.

[35] Dubois J., Jullien T., Portier F., Roche P., Cavanna A., Jin Y., Wegscheider W., Roulleau P. and Glattli D. C., *Nature*, **502** (2013) 659.

[36] Hofer P. P. and Büttiker M., *Phys. Rev. B*, **88** (2013) 241308(R).

[37] Inhofer A. and Bercioux D., *Phys. Rev. B*, **88** (2013) 235412.

[38] Hahn C., de Loubens G., Viret M., Klein O., Naletov V. V. and Ben Youssef J., *Phys. Rev. Lett.*, **111** (2013) 217204.

[39] Hyde P., Bai L., Kumar D., Southern B., Huang S. Y., Miao B. F., Chien C. L. and Hu C.-M., *Electrical detection of direct and alternating spin current injected from a ferromagnetic insulator into a ferromagnetic metal*, arXiv:1310.4840 (2013).

[40] Wei D., Obstbaum M., Back C. and Woltersdorf G., *Experimental observation of a large ac-spin Hall effect*, arXiv:1307.2961 (2013).

[41] Weiler M., Shaw J. M., Nembach H. T. and Silva T. J., *Phase-sensitive detection of spin pumping via the ac inverse spin Hall effect*, arXiv:1401.6469 (2014).

[42] Jiao H. and Bauer G. E. W., *Phys. Rev. Lett.*, **110** (2013) 217602.

[43] Kochan D., Gmitra M. and Fabian J., *Phys. Rev. Lett.*, **107** (2011) 176604.

[44] Sothmann B. and Büttiker M., *EPL (Europhys. Lett.)*, **99** (2012) 27001.

[45] Bernevig B. A., Hughes T. L. and Zhang S.-C., *Science*, **314** (2006) 1757.

[46] Liu C., Hughes T. L., Qi X.-L., Wang K. and Zhang S.-C., *Phys. Rev. Lett.*, **100** (2008) 236601.

[47] Zhang D., Lou W., M. M., Zhang S.-C. and Chang K., *Phys. Rev. Lett.*, **111** (2013) 156402.

[48] Lunde A. M. and Platero G., *Phys. Rev. B*, **88** (2013) 115411.

[49] Pfeuffer-Jeschke A., Ph.D. thesis Physikalisches Institut, Universität Würzburg (2000).

[50] König M., Buhmann H., Molenkamp L. W., Hughes T., Liu C.-X., Qi X.-L. and Zhang S.-C., *J. Phys. Soc. Jpn.*, **77** (2008) 031007.

[51] Zhou B., Lu H.-Z., Chu R.-L., Shen S.-Q. and Niu Q., *Phys. Rev. Lett.*, **101** (2008) 246807.

[52] Shevtsov O., Carmier P., Petitjean C., Groth C., Carpentier D. and Waintal X., *Phys. Rev. X*, **2** (2012) 031004.

[53] Scharf B., Matos-Abiague A. and Fabian J., *Phys. Rev. B*, **86** (2012) 075418.

[54] Chen J.-C., Wang J. and Sun Q.-F., *Phys. Rev. B*, **85** (2012) 125401.

[55] Wang Q., Liu X., Zhang H.-J., Samarth N., Zhang S.-C. and Liu C.-X., *Quantum anomalous Hall effect in magnetically doped InAs/GaSb quantum wells*, arXiv:1311.4113 (2013).